J|A|C|S COMMUNICATIONS

Published on Web 12/04/2009

Magnetolithographic Patterning of Inner Walls of a Tube: A New Dimension in Microfluidics and Sequential Microreactors

Amos Bardea,[†] Aviad Baram,[‡] Anand Kumar Tatikonda,[†] and Ron Naaman*[,†]

Department of Chemical Physics, Department of Material and Interfaces, Weizmann Institute, Rehovot 76100, Israel

Received October 12, 2009; E-mail: ron.naaman@weizmann.ac.il

An important difference between the common chemical processes occurring in solutions and chemistry in vivo lies in sequential processes typical of biological systems. Namely, in vivo, space and time are separated in reactions occurring in a sequence, whereas, in vitro, one has to separate the reactants and products physically to conduct sequential processes. This gap was bridged, however, when the concept of lab-on-a-chip (LOC) was introduced. The microfluidic technology associated with micrototal analysis systems in LOC[1−4] has been developing rapidly and will undoubtedly revolutionize the chemical, pharmaceutical, healthcare, and food industries.[5] Among others, it requires the development of surface patterning methods that allow the deposition of reactants at a well-defined spot with typically submicrometer resolution.[6−20]

In a typical LOC system, the microchannel is one of the most common and indispensable components, through which the sample's preconcentration and separation or mixing can be realized. Consequently, the results of these processes can be delivered to the desired area to execute corresponding reaction and detection tasks.[21,22] Hence, a typical LOC element has two types of components: the microchannels and the reaction/detection compartments. Here we apply the magnetolithography (ML) method,[23,24] which introduces a new feature, the patterning of the inside of a tube. This method therefore allows one to combine the two elements, the microchannel and the reaction compartments, into a third type of element, the tube reactor. Hence, it is possible, in principle, to perform all LOC chemical and biochemical reactions within the microchannel, thereby reducing production time and the amount of material that has to be processed. The new element allows one to perform sequential processes by applying a very simple and inexpensive technique.

ML is performed by patterning a magnetic field on the substrate by placing paramagnetic or diamagnetic metal masks on their backside in the presence of a constant magnetic field. The mask defines the spatial distribution and shape of the magnetic field applied on the substrate. The second component in ML is ferromagnetic nanoparticles (NPs) that reside on the substrate according to the field induced by the mask. ML can be applied in either the positive or negative mode. In the positive mode, the magnetic NPs react chemically or interact via chemical recognition with the substrate. Hence, the magnetic NPs are immobilized at selected locations, where the mask induces a magnetic field, resulting in a patterned substrate. In the negative mode, the magnetic NPs do not interact chemically with the substrate. Hence, once they pattern the substrate, they block their site on the substrate. The exposed areas, not covered by the NPs, can at this stage be covered by molecules that chemically bind to the substrate. After the binding of these molecules, the NPs are removed, resulting in a "negatively" patterned substrate. ML is a backside lithography process that does not depend on the surface topography and planarity; therefore, ML allows the chemical patterning of the inside of tubes.

Here, we show the capabilities of ML for patterning the inside of tubes by demonstrating positive and negative ML processes and sequential reactions made possible by these processes.

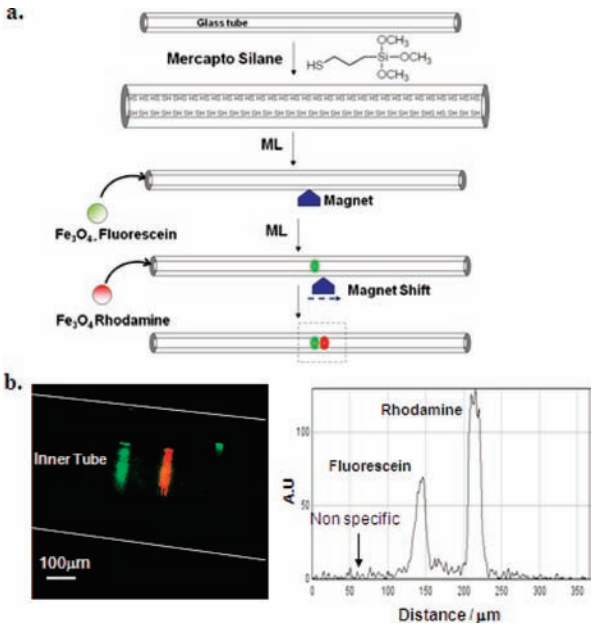

Figure 1. (a) Scheme describing the patterning of the inner tube surface by applying positive magnetolithography. (b) Fluorescence of both fluorescein and sulforhodamine observed from the two bands of the nanoparticles adsorbed within the tube. (c) Profile of the fluorescence signal shown in b.

Figure 1 shows positive ML when the inner surface of glass tube was functionalized with mercapto silan by immersed mercapto propyl trimethoxy silane in bicyclohexyl (BCH). Magnetic NPs (Fe_3O_4) with a 10 nm diameter were coated by fluorescein and sulforhodamine. A magnetic field was applied on the tube by using a permanent magnet. The fluorescein-labeled magnetic NPs were injected into the tube and adsorbed at the sites at which the magnetic field gradient was maximal. The tube was washed with ethanol, and the magnetic field was shifted to another site. Next, sulforhodamine-labeled magnetic NPs were injected into the tube, concentrating at the new site. This process resulted in two fluorescence bands, as shown in Figure 1b. Figure 1c shows the profile of the fluorescence signal. The nonspecific adsorption is ∼5% relative to the specific one.

Figure 2 presents a scheme for negative ML. The inner part of a glass tube was functionalized by amino propyl trimethoxy silane (step 1). Then a magnetic field of 100 G was applied at one site along the tube, and a solution containing Fe_3O_4 NPs was injected into the tube (step 2). The size of the field was chosen so as to reduce the nonspecific adsorption of the NPs. The NPs concentrate as a ring at the site at which the magnetic field is applied. In the

[†] Department of Chemical Physics.
[‡] Department of Material and Interfaces.

10.1021/ja908675c

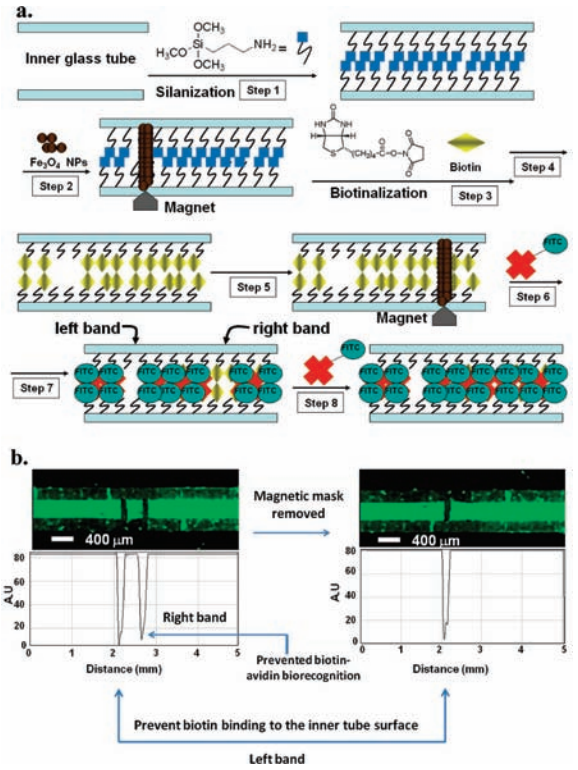

Figure 2. (a) Scheme describing the stepwise surface patterning of the inner surface of a tube by applying negative magnetolithography. (b) Fluorescence observed from a tube patterned by the negative magnetolithography process, as described in a.

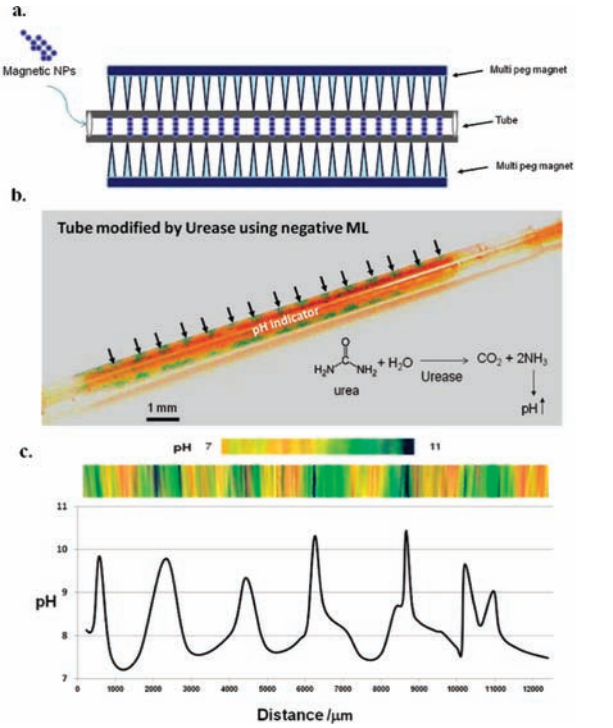

Figure 3. (a) Scheme describing the multipeg magnet for applying ML in the tube. (b) Color of a pH indicator flushed in a solution of urea and pH indicator through a tube patterned with the enzyme urease. (c) Change in pH along the tube, as obtained from the variation of the indicator's color.

next step, a solution of *N*-hydroxy-succinimide-biotin (NHS-biotin) was reacted with the amino functional patterned surface. The site covered with the NPs is protected and therefore does not react with the NHS-biotin (step 3). This process results in selective locations for biotinilation at the surface, which were not covered with the NPs. Since the magnetic NPs are inert to the surface, they can easily be removed by washing the surface after the magnetic mask is removed (step 4). To demonstrate the success of the multiple-stage patterning of the inner surface of the tube, we exposed the biotinilated tube to a magnetic field at a second location. NPs were injected into the tube (step 5). Again, the magnetic NPs were driven by the magnetic field and assembled at the new site. The substrate was then exposed to a buffer phosphate solution (pH 8) of fluorophore-labeled avidin (Av-FITC) (step 6). Hence, the biotin groups underneath the NPs were protected and did not interact with the Av-FITC. This negative ML process resulted in a patterned surface with two bands detected by a Fujifilm FLA-5100 scanner (see Figure 2b). The left band represents the negative ML, where a reaction between biotin-NSH molecules and the amine group in the inner tube surface is prevented, whereas the right band results from NPs that prevented the interaction between the already adsorbed biotin molecules and Av-FITC in the solution. The second negative ML process is reversible, since removing the magnet causes the magnetic NPs to be released (step 7). Consequently, the biotin groups at these sites are deprotected and now Av-FITC molecules that are injected into the tube can interact with the adsorbed biotin groups (step 8), as shown in Figure 2b.

To date, we demonstrated the ability to pattern the inner surface of a tube with relatively small molecules. However, for sequential processes, the reaction between the reactant in the solution and the one adsorbed on the surface must be localized. Next, we will demonstrate the ability to pattern the inner part of the tube with enzyme and reveal the localization of the reaction (Figure 3). Here, the enzyme urease was patterned on the inside of the 500 μm diameter tube at different places using the negative ML approach.

First, the inner surface of the tube was modified by amino propyl trimethoxy silane. The tube was immersed in a methanol solution. Next, the tube was exposed to a multipeg magnet that induced a magnetic field of 100 G, and a solution magnetic NPs was injected into the tube. The magnetic NPs were arranged along the tube according to the magnetic field induced by the magnetic pegs as shown in Figure 3a. The covalent coupling of urease to the amino propyl silan was performed by injecting an HEPES buffer solution, pH 7.3 containing 0.5 mg mL^{-1} urease in the presence of 0.01 M 1-ethyl-3-(3-(dimethylamino)propyl)carbodiimide (EDC). Consequently, the urease covalently bound to the amine groups that were not protected by the magnetic NPs. The NPs were removed by washing the tube. A solution containing 0.1 M urea and a pH indicator was flushed through the tube. At the regions where the urease was patterned, the enzyme decomposed the urea, producing NH_3. As a result, the pH in that region increased and the indicator changed its color to green/blue at urease binding sites. As is clearly shown in Figure 3b, the high pH regions appear as green spots inside the tube. The pH variation along the tube can be analyzed, based on the change in the color of the indicator, and is shown in Figure 3c.

After demonstrating the ability to achieve localized enzymatic reactions inside the tube, we applied negative ML for sequential enzymatic reactions. Here, the proteins glucose oxidase (GOx) and horseradish peroxidase (HRP) were adsorbed at well-defined sites on the inner surface of the tube, as shown in Figure 4. First, the inner surface of the tube was modified by amino propyl trimethoxy silane. Next, the tube was exposed to a multipeg magnet-induced magnetic field of 100 G after which magnetic NPs were injected into the tube. The magnetic NPs arranged themselves along the tube according to the magnetic field. The covalent coupling of GOx to the amino groups that were not protected by the magnetic NPs was performed by

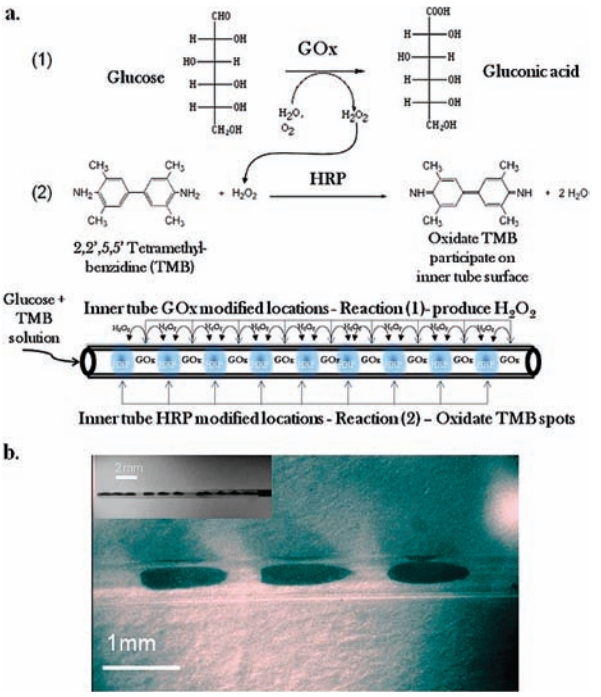

Figure 4. (a) Scheme of sequential enzymatic reactions inside the tube obtained by patterning proteins glucose oxidase (GOx) and horseradish peroxidase (HRP) on the inner surface of the tube. (b) The participate oxidate TMB, resulting from the sequential reaction, is seen as dark spots.

injecting a buffer solution containing GOx in the presence of EDC. Consequently, the GOx covalently bound to those amine groups that were not protected by the magnetic NPs. The NPs were removed by washing the tube. Next, we performed a second cycle of ML to protect the GOx binding sites by magnetic NPs using a multipeg magnet that induced the magnetic field at the GOx binding sites. Then, the covalent coupling of HRP to amino propyl silane was performed by injecting a buffer solution containing HRP in the presence of EDC. Consequently, the HRP covalently bound to the amine groups, which are located in-between GOx binding sites.

The sequential enzymatic reaction in the tube was initiated by injecting glucose with 2,2,5,5′-tetramethyl-benzidine (TMB). The GOx was biocatalyzed by the oxidation of glucose, yielding gluconic acid and H_2O_2. The H_2O_2 diffused to the HRP binding site and there the HRP biocatalyzed the oxidation of TMB by H_2O_2, yielding an insoluble product. Figure 4b shows the results of the sequential enzymatic reactions indicated by spots generated by participates of insoluble products at the location of the HRP.

The localization of the patterned GOx was demonstrated in controlled experiments. To observe the binding sites of the GOx in the tube, we conjugated to Alexa 488 fluorophore. The GOx protein was labeled with Alexa carboxylic acid and purified according to the Invitrogen Alexa Fluor 488 protein labeling procedure. The GOx binding sites were detected by a Fujifilm FLA-5100 scanner. The result, shown in Figure 5, proves that it is possible to localized GOx and HRP in separate regions onto the inner surface of the tube.

In addition a set of controlled experiments proved that the insoluble product is generated only when all components exist, namely, when both GOx and HRP are adsorbed and glucose and TMB are dissolved in the solution.

Here we demonstrated the ability to pattern the inside of a tube and to use the patterned substrate for catalyzing reactions in spatially

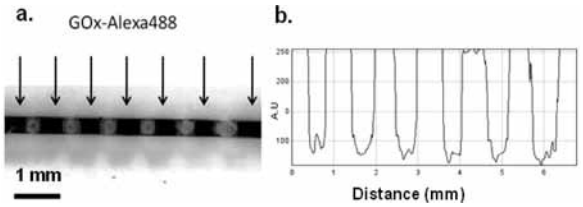

Figure 5. (a) Image obtained from Alexa-labeled GOx adsorbed on selected sites at the inner surface of the tube. (b) Chart of the fluorescence intensity profile along the tube.

localized regions. For visualization reasons, we did not attempt to reduce the spatial resolution below that of hundreds of micrometers, but as was demonstrated before, the ML provides the ability to obtain resolution on a scale of tens of nanometers.[25] The new abilities demonstrated here open up the possibility of inducing chemical and biochemical patterning of the inner tube surfaces, especially when using tubes with a small diameter as efficient reactors for LOC and for DNA sequencing.

Acknowledgment. Partial support was obtained from the Grand center and from the Helen and Martin Kimmel Center for Nanoscale Science.

Supporting Information Available: Supporting methods that complement the article are available. This material is available free of charge via the Internet at http://pubs.acs.org.

References

(1) Andersson, H.; Berg, A. V. D. *Lab-on-Chips for Cellomics: Micro and Nanotechnologies for Life Science*; Kluwer Academic: London, 2004; pp 171−196.
(2) Geschk, O.; Klank, H.; Telleman, P. *Microsystem Engineering of Lab-on-a-Chip Devices*; Wiley-VCH: Weinheim, 2008; pp 1−7.
(3) Weigl, B. H.; Bardell, R. L.; Cabrera, C. R. *Adv. Drug Delivery* **2003**, *55*, 349–377.
(4) Daniel, F.; Devanand, P. *Anal. Chem.* **2000**, *72*, 330–335.
(5) Craighead, H. *Nature* **2006**, *442*, 387–393.
(6) Boal, A. K.; Ilhan, F.; DeRouchey, J. E.; Thurn-Albrecht, T.; Russell, T. P.; Rotello, V. M. *Nature* **2000**, *404*, 746–748.
(7) Cox, J. K.; Eisenberg, A.; Lennox, R. B. *Curr. Opin. Colloid Interface Sci.* **1999**, *4*, 52–59.
(8) Higgins, A. M.; Jones, R. A. L. *Nature* **2000**, *404*, 476–478.
(9) Jacobs, H. O.; Tao, A. R.; Schwartz, A.; Gracias, D. H.; Whitesides, G. M. *Science* **2002**, *296*, 323–325.
(10) Terris, B. D.; Thomson, T. *J. Phys. D: Appl. Phys.* **2005**, *38*, R199–R222.
(11) Martinez, R. V.; Losilla, N. S.; Martinez, J.; Tello, M.; Garcia, R. *Nanotechnol.* **2007**, *18*, 0844021.
(12) Hong, S.; Mirkin, C. A. *Science* **2000**, *288*, 1808–1811.
(13) Zhang, H.; Amro, N. A.; Disawal, S.; Elghanian, R.; Shile, R.; Fragala, J. *Small* **2007**, *3*, 81–85.
(14) Salaita, K.; Wang, Y.; Fragala, J.; Vega, R. A.; Liu, C.; Mirkin, C. A. *Angew. Chem.* **2006**, *45*, 7220–7223.
(15) Stewart, M. E.; Motala, M. J.; Yao, J.; Thompson, L. B.; Nuzzo, R. G. J. *Nanoengineering and Nanosystems* **2007**, *220*, 81–138.
(16) Hoeppener, S.; Maoz, R.; Sagiv, J. *Nano Lett.* **2003**, *3*, 761–767.
(17) Buxboim, A.; Bar-Dagan, M.; Frydman, V.; Zbaida, D.; Morpurgo, M.; Bar-Ziv, R. *Small* **2007**, *3*, 500–510.
(18) (a) Quist, A. P.; Pavlovic, E.; Oscarsson, S. *Anal. Bioanal. Chem.* **2005**, *381*, 591–600. (b) Xu, C.; Taylor, P.; Ersoz, M.; Fletcher, P. D. I.; Paunov, V. N. *J. Mater. Chem.* **2003**, *13*, 3044–3048. (c) Lange, S. A.; Benes, V.; Kern, D. P.; Horber, J. K. H.; Bernard, A. *Anal. Chem.* **2004**, *76*, 1641–1647. (d) Schmalenberg, K. E.; Buettner, H. M.; Uhrich, K. E. *Biomaterials* **2004**, *25*, 1851–1857.
(19) (a) Geissler, M.; Bernard, A.; Bietsch, A.; Schmid, H.; Michel, B.; Delamarche, E. *J. Am. Chem. Soc.* **2000**, *122*, 6303–6304. (b) Michel, B.; Bernard, A.; Bietsch, A.; Delamarche, E.; Geissler, M.; Juncker, D.; Kind, H.; Renault, J. P.; Rothuizen, H.; Schmid, H.; Schmidt-Winkel, P.; Stutz, R.; Wolf, H. *IBM J. Res. Dev.* **2001**, *45*, 697–719.
(20) Couderc, S.; Blech, V.; Kim, B. J. J. *Appl. Phys.* **2009**, *48*, 095007.
(21) Li, P. C. H. *Microfluidic Lab-on-a-Chip for Chemical and Biological Analysis and Discovery*; Taylor & Francis Group, LLC: 2006; pp 1−2.
(22) Medoro, G.; Manaresi, N.; Leonardi, A.; Altomare, L.; Tartagni, M.; Guerrieri, R.; Labon, A. *IEEE Sens. J.* **2003**, *3*, 317–325.
(23) Bardea, A.; Naaman, R. *Small* **2009**, *5*, 316–319.
(24) Yellen, B. B.; Fridman, G.; Friedman, G. *Nanotechnology* **2004**, *15*, S562–S565.
(25) Bardea, A.; Naaman, R. *Langmuir* **2009**, *25*, 5451–5454.

JA908675C